The Effect of Wind on Ground-Tracker Quadcopter

October 21, 2018

1 Introduction

The rise of quadcopters caused a lot of interest in the controlling of it, because, in contrast with traditional flight systems, quadcopters are not based on sophisticated theories, but uses the concept of four rotors along with controllers to fly. As a result, there are some physical effects that were not studied thoroughly. One of them is the effect of the presence of wind on the quadcopter, although the effect of wind on rotors was studied, mainly with focus on helicopters. Because of the fact that a simple quadcopter has four rotors, it is possible to control only four states of the quadcopter, and many controllers can be developed.

The purpose of this paper is to look forward on the effect of wind on a quadcopter. The study is done on a simple quadcopter that has a PD controller on its attitude and altitude, and is based on SIMULINK simulation of it. It includes a full modeling of a quadopter and a controller for it, and the study of its basic dynamics, modeling of the effect of wind on the quadcopter and simulation of it.

Chapters 2 through 6 show the study of the quadcopter without the presence of wind, chapters 7 and 8 focus on the wind and its effect, and chapter 9 show the simulation results.

2 Modeling a Quadcopter in Simulink

In this work, SIMULINK was used in order to simulate a quadcopter. The simulation was based on [Luukkonen, 2011], which derived the model for a quadcopter with 4 rotors. The dynamic model that was derived is applicable for any number of rotors that is a multiplication of 4, which is what was used in this paper. The dynamic model of the quadcopter consists six degrees of freedom: $\xi = [x, y, z]$, which is the spatial location of the quadcopter in inertial coordinate system, and $\eta = [\phi, \theta, \psi]$, which are the euler angles of the quadcopter with respect to the inertial reference system. The dynamics of the quadcopter are described using the following equations, expressed using p, q, r, the angular rates of the quad in it's coordinate system:

$$\begin{bmatrix} \dot{p} \\ \dot{q} \\ \dot{r} \end{bmatrix} = \begin{bmatrix} (I_{yy} - I_{zz})qr/I_{xx} \\ (I_{zz} - I_{xx})pr/I_{yy} \\ (I_{xx} - I_{yy})pq/I_{zz} \end{bmatrix} - I_r \begin{bmatrix} q/I_{xx} \\ -p/I_{yy} \\ 0 \end{bmatrix} \omega_\Gamma + \begin{bmatrix} \tau_\phi/I_{xx} \\ \tau_\theta/I_{yy} \\ \tau_\psi/I_{zz} \end{bmatrix} \tag{1}$$

$$\begin{bmatrix} \dot{\phi} \\ \dot{\theta} \\ \dot{\psi} \end{bmatrix} = \begin{bmatrix} 1 & S_\phi T_\theta & C_\phi T_\theta \\ 0 & C_\phi & -S_\phi \\ 0 & S_\phi/C_\theta & C_\phi/C_\theta \end{bmatrix} \begin{bmatrix} p \\ q \\ r \end{bmatrix} \tag{2}$$

$$\begin{bmatrix} \ddot{x} \\ \ddot{y} \\ \ddot{z} \end{bmatrix} = -g \begin{bmatrix} 0 \\ 0 \\ 1 \end{bmatrix} + \frac{1}{m} \begin{bmatrix} C_\psi S_\theta C_\phi + S_\psi S_\phi \\ S_\psi S_\theta C_\phi - C_\psi S_\phi \\ C_\theta C_\phi \end{bmatrix} T - \frac{1}{m} \begin{bmatrix} A_x & 0 & 0 \\ 0 & A_y & 0 \\ 0 & 0 & A_z \end{bmatrix} \begin{bmatrix} \dot{x} \\ \dot{y} \\ \dot{z} \end{bmatrix} \tag{3}$$

In these equations, m is the quadcopter mass, g is the gravitational acceleration, I_{xx}, I_{yy} and I_{zz} are the moments of inertia of the quadcopter around it's coordinate system, and I_r is the rotor's moment of inertia in it's own coordinate system. T is the total thrust that is created by the rotors, and is given by:

$$T = \sum_{i=1}^{N} k \cdot \omega_i^2 \tag{4}$$

where ω_i is the angular velocity of the i'th quadcopter, k is the lift constant, which will be inspected in later chapters and $\omega_\Gamma = \sum_{i=1}^{N} \omega_i$. τ_ϕ, τ_θ and τ_ψ are the moments created on the quadcopter from the rotors, expressed in the quadcopter coordinate system. In this report, we changed the configuration of the rotors so that the x-axis will be directed between two rotors. They are given by the following equations:

$$\begin{bmatrix} \tau_\phi \\ \tau_\theta \\ \tau_\psi \end{bmatrix} = \begin{bmatrix} \sum_{i=1}^{N} -lk\omega_i^2 sin(\theta_i) \\ \sum_{i=1}^{N} -lk\omega_i^2 cos(\theta_i) \\ \sum b \cdot \omega_i \cdot |\omega_i| \end{bmatrix} \tag{5}$$

where l is the distance of the rotors from the center of gravity of the quadcopter (this is assumed to be equal in all rotors, i.e. the quadcopter body is symmetric), b is the drag constant, and θ_i is the angle between the i's rotor and the x-axis. In the four-rotors X configuration, $\theta_1 = 45^\circ, \theta_2 = 135^\circ, \theta_3 = 225^\circ, \theta_4 = 315^\circ$.

It is assumed here that $I_{xx} = I_{yy}$, which is true in any case where the rotors are symmetric. The rotors are planned so that ω_1, ω_3 are always positive and ω_2, ω_4 are always negative.

A_x, A_y and A_z are drag coefficients, so in this case we consider drag that is proportional to the velocity.

3 Calculating the equilibriom point

Analyzing the dynamic response of a quadcopter, starts with finding an equilibrium point and the constraints on it.

In equilibria, the accelerations and angular rates vanish. We will also demand that the velocity will be 0. This assumption will become important when we'll consider the aerodynamic effects. Under these conditions, equation 1 suggests:

$$\begin{bmatrix} \tau_\phi \\ \tau_\theta \\ \tau_\psi \end{bmatrix} = \begin{bmatrix} \sum_{i=1}^{N} -lk\omega_i^2 sin(\theta_i) \\ \sum_{i=1}^{N} -lk\omega_i^2 cos(\theta_i) \\ \sum b \cdot \omega_i \cdot |\omega_i| \end{bmatrix} = 0 \tag{6}$$

and equation 3 suggests (using equation 4):

$$-g + \frac{\sum_{i=1}^{N} k \cdot \omega_i^2}{m} cos(\theta)cos(\phi) = 0 \tag{7}$$

From the two upper equations we conclude that $\theta = \phi = 0$ (here we assumed that the velocity is 0).

For four rotors, we can solve these equations analytically. First, we will decide apriori that the direction of rotation of even rotors will be opposite to the direction of the odd rotors (This decision allows us to zero the torque around the z axis). The equations on the torques suggest:

$$\omega_1 = \omega_3 = -\omega_2 = -\omega_4 = \omega \tag{8}$$

Using the 4'th equation, we get $-g + \frac{4k \cdot \omega^2}{m} = 0$ so that

$$\omega = \sqrt{\frac{mg}{4k}} \tag{9}$$

4 Linearization

4.1 Linearization in State-Space

Each of the equations that were presented in chapter 2 contains nonlinearity. One way to understand the basic behavior of the model is to linerize it. First, we define state-space model for the system. Defining X, Y, Z as the location of the quadcopter in space (inertial frame), U, V, W the velocity of the quadcopter in the corresponding axes, P, Q, R, the angular rates in body axes, and Ψ, Θ, Φ the euler angles of the quadcopter. The first case that will be examined is trim in hovering, which was calculated in chpater 3. Thus, $X_0 = Y_0 = Z_0 = 0$, $U_0 = V_0 = W_0 = 0$, $P_0 = Q_0 = R_0 = 0$ and $\Psi_0 = \Theta_0 = \Phi_0 = 0$. Inputs are $\Omega_1 = \Omega_3 = -\Omega_2 = -\Omega_4 = \sqrt{\frac{mg}{4k}}$. The outputs of the system will be X, Y, Z and Ψ, Θ, Φ. Small perturbations of trim will be noted by $\Delta X, \Delta Y, \Delta Z$, $u, v, w, p, q, r, \psi, \theta, \phi$, and $\omega_1, \omega_2, \omega_{3,}\omega_4$ for the inputs. We calculate state-space linearized system of the perturbations using the following formulas:

$$A = [A_{ij}]_{1 \le i,j \le N} = [\frac{\partial f_i}{\partial x_j}]_0 \tag{10}$$

$$B = [B_{ij}]_{1 \le i \le N, 1 \le j \le M} = [\frac{\partial f_i}{\partial u_j}]_0 \tag{11}$$

$$C = [C_{ij}]_{1 \le i \le L, 1 \le j \le N} = [\frac{\partial y_i}{\partial x_j}]_0 \tag{12}$$

$$D = [D_{ij}]_{1 \le i \le L, 1 \le j \le M} = [\frac{\partial y_i}{\partial u_j}]_0 \tag{13}$$

where '0' denotes trim conditions, f_i is the equation defining $\dot{x}_i$, and y_i is the equation defining the i'th output.

$$A = \begin{bmatrix} 0 & 0 & 0 & 1 & 0 & 0 & 0 & 0 & 0 & 0 & 0 & 0 \\ 0 & 0 & 0 & 0 & 1 & 0 & 0 & 0 & 0 & 0 & 0 & 0 \\ 0 & 0 & 0 & 0 & 0 & 1 & 0 & 0 & 0 & 0 & 0 & 0 \\ 0 & 0 & 0 & -\frac{A_x}{m} & 0 & 0 & 0 & 0 & 0 & 0 & g & 0 \\ 0 & 0 & 0 & 0 & -\frac{A_y}{m} & 0 & 0 & 0 & 0 & 0 & 0 & -g \\ 0 & 0 & 0 & 0 & 0 & -\frac{A_z}{m} & 0 & 0 & 0 & 0 & 0 & 0 \\ 0 & 0 & 0 & 0 & 0 & 0 & 0 & 0 & 0 & 0 & 0 & 0 \\ 0 & 0 & 0 & 0 & 0 & 0 & 0 & 0 & 0 & 0 & 0 & 0 \\ 0 & 0 & 0 & 0 & 0 & 0 & 0 & 0 & 0 & 0 & 0 & 0 \\ 0 & 0 & 0 & 0 & 0 & 0 & 0 & 0 & 1 & 0 & 0 & 0 \\ 0 & 0 & 0 & 0 & 0 & 0 & 0 & 1 & 0 & 0 & 0 & 0 \\ 0 & 0 & 0 & 0 & 0 & 0 & 1 & 0 & 0 & 0 & 0 & 0 \end{bmatrix}$$

$$B = \begin{bmatrix} 0 & 0 & 0 & 0 \\ 0 & 0 & 0 & 0 \\ 0 & 0 & 0 & 0 \\ 0 & 0 & 0 & 0 \\ 0 & 0 & 0 & 0 \\ \sqrt{\frac{gk}{m}} & -\sqrt{\frac{gk}{m}} & \sqrt{\frac{gk}{m}} & -\sqrt{\frac{gk}{m}} \\ -\frac{1}{I_{xx}}\sqrt{\frac{l^2mgk}{2}} & \frac{1}{I_{xx}}\sqrt{\frac{l^2mgk}{2}} & \frac{1}{I_{xx}}\sqrt{\frac{l^2mgk}{2}} & -\frac{1}{I_{xx}}\sqrt{\frac{l^2mgk}{2}} \\ -\frac{1}{I_{yy}}\sqrt{\frac{l^2mgk}{2}} & -\frac{1}{I_{yy}}\sqrt{\frac{l^2mgk}{2}} & \frac{1}{I_{yy}}\sqrt{\frac{l^2mgk}{2}} & \frac{1}{I_{yy}}\sqrt{\frac{l^2mgk}{2}} \\ \frac{b}{I_{zz}}\sqrt{\frac{mg}{k}} & \frac{b}{I_{zz}}\sqrt{\frac{mg}{k}} & \frac{b}{I_{zz}}\sqrt{\frac{mg}{k}} & \frac{b}{I_{zz}}\sqrt{\frac{mg}{k}} \\ 0 & 0 & 0 & 0 \\ 0 & 0 & 0 & 0 \\ 0 & 0 & 0 & 0 \end{bmatrix}$$

$$C = \begin{bmatrix} 1 & 0 & 0 & 0 & 0 & 0 & 0 & 0 & 0 & 0 & 0 & 0 \\ 0 & 1 & 0 & 0 & 0 & 0 & 0 & 0 & 0 & 0 & 0 & 0 \\ 0 & 0 & 1 & 0 & 0 & 0 & 0 & 0 & 0 & 0 & 0 & 0 \\ 0 & 0 & 0 & 0 & 0 & 0 & 0 & 0 & 0 & 1 & 0 & 0 \\ 0 & 0 & 0 & 0 & 0 & 0 & 0 & 0 & 0 & 0 & 1 & 0 \\ 0 & 0 & 0 & 0 & 0 & 0 & 0 & 0 & 0 & 0 & 0 & 1 \end{bmatrix}$$

and $D = 0$.

The transfer function from the input to the x and y-location of the quadcopter is:

$$\frac{a}{s^4 + \beta s^3}$$

showing that a small perturbation in the angular velocity of the rotor can cause the quadcopter location to diverge. The transfer function to the z location has one less integrator and the constant a is different. The transfer function to the euler angles is:

$$\frac{c}{s^2}$$

which shows that it can also cause a divergion of euler angles. All the transfer functions have different signs as function of the number of the rotor.

4.2 Transfer Functions and the System Poles

After linearizing the equations, it is possible to find the poles of the system. The poles of equations (1) and (2) are in the origin, which tells us that the system diverges with small perturbations. The transfer function from euler angles ϕ and θ to y and x, consequently, and the transfer function from the thrust T to z coordinate, have a pole in the origin and a pole in the OLHP. This also tells us that they diverge with small perturbations. Indeed, simulation of the quadcopter with small perturbations in initial conditions and angular velocity is showed in figures 1 and 2, which shows divergence with time of the loaction of the quadcopter (the velocity arrives steady-state in this period, because an initial condition is equivalent to a delta perturbation). The linearization leads to the understanding that a quadcopter needs a control system in order to be stabilized.

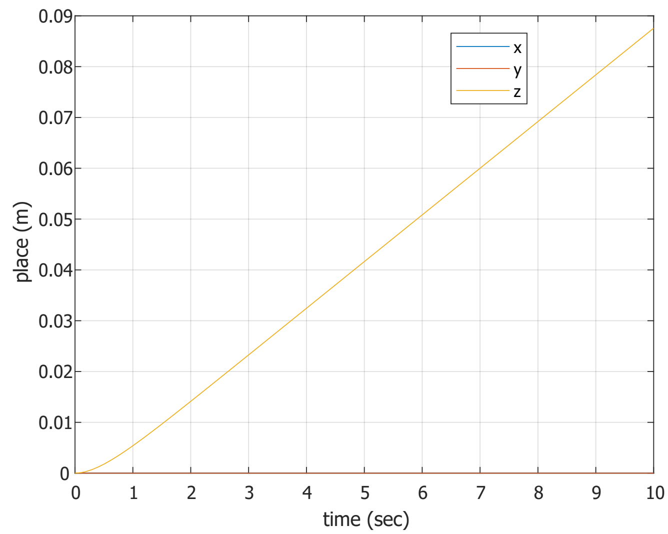

Figure 1: Location of quadcopter in time, with $\omega = \omega^* \cdot 1.001$

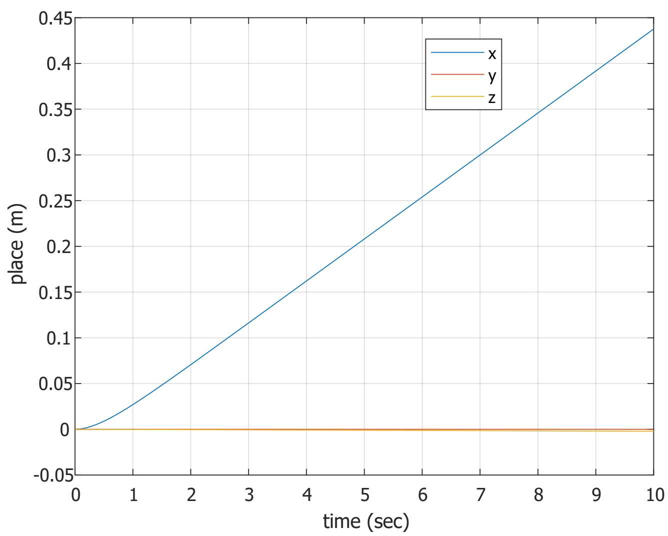

Figure 2: Location of quadcopter in time, with $\theta_0 = 0.01rad$

5 Stabilizing the quadcopter with constant speed

Next, we want to stabilize the quadcopter with constant speed. We allow the velocity to be nonzero only in x axis. The only thing that changes is the euler angles, in order to satisfy equation (3). Thus, the torques remain the same, and equation (8) holds. Setting $\psi = 0$ and $\phi = 0$, we get

$$\frac{T}{m} sin(\theta) = \frac{A_x}{m}\dot{x} \tag{14}$$

The last equation is the third element in equation (3), which leads to:

$$\frac{T}{m} cos(\theta) = g \tag{15}$$

Dividing (14) by (15) we get $tan(\theta) = \frac{A_x}{mg}\dot{x}$ and therefore

$$\theta = arctan(\frac{A_x}{mg}\dot{x}) \tag{16}$$

Substituting into (15) we get $T = \frac{mg}{cos(arctan(\frac{A_x}{mg}\dot{x}))}$ and so:

$$\omega = \sqrt{\frac{mg}{4kcos(arctan(\frac{A_x}{mg}\dot{x}))}} \tag{17}$$

5.1 Simulation results

The velocity was set to $\dot{x} = 1.5\frac{m}{s}$ and initial conditions to $\dot{x} = 1\frac{m}{s}$, $\dot{y} = 0.5\frac{m}{s}$ and $\dot{z} = 0.1\frac{m}{s}$, $\phi = \psi = 0$ and $\theta = arctan(\frac{A_x}{mg}\dot{x})$, and setting the control angular velocity as in equation (17). The simulation results are shown in figure 3. It can be seen that the x element of the velocity reaches steady-state at the velocity that was calculated, and the velocities in the other axes vanish in steady state, as a result of the aerodynamic forces.

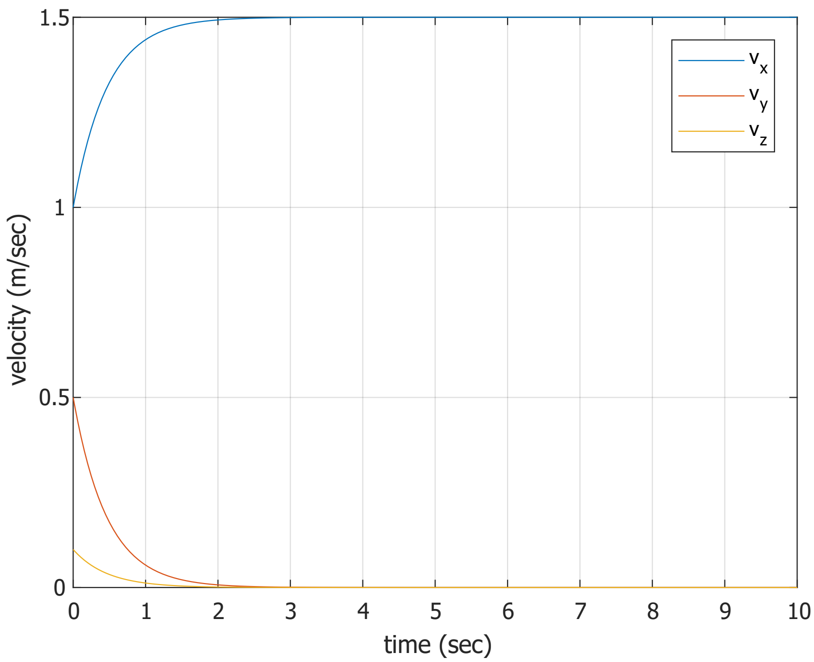

Figure 3: Velocity of quadcopter in inertial frame

6 Basic Controllers to Stabilize the Quadcopter

6.1 The Contoller

Our quadcopter has 4 degrees of freedom, and therefore we will be able to control on 4 states. Here we'll use the controller developed in [Luukkonen, 2011], which is a proportional and derivative controllers for each input of the equations of motion of the quadcopter, and then translate it to the angular rates that correspond.

$$T = (g + K_{z,D}(\dot{z}_c - \dot{z}) + K_{z,P}(z_c - z))\frac{m}{C_\phi C_\theta} \tag{18}$$

$$\tau_\phi = (K_{\phi,D}(\dot{\phi}_c - \dot{\phi}) + K_{\phi,P}(\phi_c - \phi))I_{xx} \tag{19}$$

$$\tau_\theta = (K_{\theta,D}(\dot{\theta}_c - \dot{\theta}) + K_{\theta,P}(\theta_c - \theta))I_{yy} \tag{20}$$

$$\tau_\psi = (K_{\psi,D}(\dot{\psi}_c - \dot{\psi}) + K_{\psi,P}(\psi_c - \psi))I_{zz} \tag{21}$$

where $z_c, \phi_c, \theta_c, \psi_c$ are the input signals, and $K_{\bullet,d/P}$ are the controllers constants. Inverting equations (4) and (5) (that are linear in ω_i^2) leads to the angular velocities needed:

$$\omega_1 = \sqrt{-\frac{\sqrt{2}\tau_\phi}{4 \cdot l \cdot k} - \frac{\sqrt{2}\tau_\theta}{4 \cdot l \cdot k} + \frac{\tau_\psi}{4b} + \frac{T}{4k}} \tag{22}$$

$$\omega_2 = -\sqrt{-\frac{\sqrt{2}\tau_\phi}{4 \cdot l \cdot k} + \frac{\sqrt{2}\tau_\theta}{4 \cdot l \cdot k} - \frac{\tau_\psi}{4b} + \frac{T}{4k}} \tag{23}$$

$$\omega_3 = \sqrt{\frac{\sqrt{2}\tau_\phi}{4 \cdot l \cdot k} + \frac{\sqrt{2}\tau_\theta}{4 \cdot l \cdot k} + \frac{\tau_\psi}{4b} + \frac{T}{4k}} \tag{24}$$

$$\omega_4 = -\sqrt{\frac{\sqrt{2}\tau_\phi}{4 \cdot l \cdot k} - \frac{\sqrt{2}\tau_\theta}{4 \cdot l \cdot k} - \frac{\tau_\psi}{4b} + \frac{T}{4k}} \tag{25}$$

6.2 Linearization

Linearizing the model of the quadcopter showed that it is not stable, having poles in the origin. After using the controllers, we checked the transfer functions of the system and verified that it is stable. We linearized and calculated the transfer functions between z, ψ, θ and ϕ to $z_c, \psi_c, \theta_c, \phi_c$, using SIMULINK's linearization tool. The results show that all of the poles are in the OLHP, which means that the quadcopter can be stabilized by simple PI controllers.

7 The Effect of Wind on the Quadcopter Thrust

[Iosilevskii] analyzed the thrust generated by a rotor, and the effect of wind in the direction of the rotor angular velocity on it. The main result for k, the lift constant presented in chapter 2 suggests:

$$k = \rho\pi R^4 c_T \tag{26}$$

where

$$c_T = k_t\frac{\sigma a}{4}(\frac{2}{3}\theta_{3/4} - \frac{1}{2}(v_s - \frac{\sigma a}{8}) - \sqrt{\frac{1}{4}(v_s - \frac{\sigma a}{8})^2 + \frac{\sigma a}{12}\theta_{3/4}}) \tag{27}$$

In equations (26) and (27), v_s is the wind velocity normal to the rotor plane which is normalized in the rotor's angular velocity: $v_s = \frac{V_s}{\Omega R}$. ρ is the air density, R is the rotor radius, k_t is an empirical constant representing the relative part of the rotor disk generating the thrust, σ is the rotor's solidity portion, a is the blade's lift line slope, $\theta_{3/4} = \theta_0 - \frac{3}{4}\theta_1$, θ_0 is the pitch angle of the blade in its root and θ_1 is the torsion per distance (normalized in radius). This formula allows us to simulate the response of the quadcopter to wind in SIMULINK. Characteristic values of these parameters are shown in table 1. An interesting observation is that wind does not have a divering behavior; if there is wind in the positive z direction of the rotor, it causes the thrust to grow, so it gets a velocity in the positive z direction, but this velocity causes the effective wind velocity on the rotor to decrease and hence the effect of the wind to decrease. The same holds for wind in the opposite direction.

ρ	$1.225\ kg/m^3$
R	$0.0905\ m$
k_t	1
σ	0.1
a	5.7 1/rad
θ_0	15 deg
θ_1	2 deg

Table 1: Characteristic values of wind model

8 Wind

This work examines the effect of wind on the performance of the quadcopter. For this purpose, we modeled the wind that the quadcopter see using Dryden model [Hoblit, 1998]. Dryden model is a turbulence model that assumes the space has a constant wind in time, and the wind that the aircraft experiences results from the aircraft's speed through the space.

The model of the wind in space is based on white noise passed through a band-limited filter. As shown in [Hoblit, 1998], the PSD of the longitudinal wind is given by:

$$\Phi_u(\omega) = \frac{2\sigma_u^2 L_u}{\pi V} \cdot \frac{1}{1 + (L_u \frac{\omega}{V})^2} \tag{28}$$

Lateral and vertical wind PSD's have the same form but have another pole and a zero. The parameter that affects the wind power is the wind speed at 6m altitude. In figure 4, a representing wind created by SIMULINK's Dryden model, for an aircraft flying in approximately $6\frac{m}{s}$ in $50m$ altitude, for which the wind speed in 6m altitude is chosen to be $5\frac{m}{s}$.

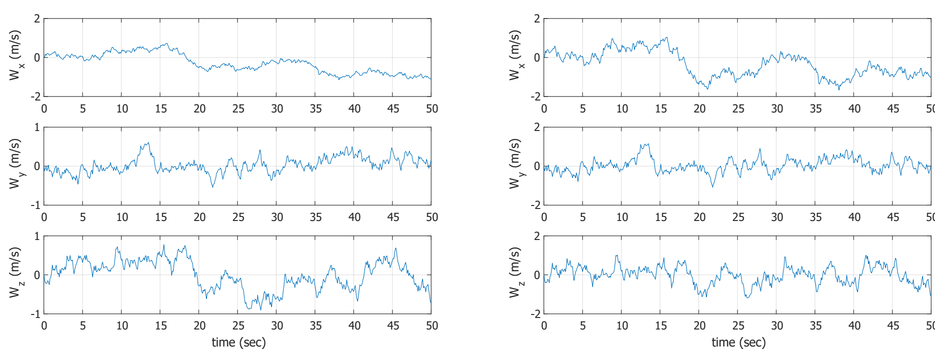

Figure 4: Wind Dryden velocity in earth's coordinate system, wind speed at 6m is $6\frac{m}{s}$, aircraft speed is $6m/s$ on left and 25 m/s on right, and aircraft altitude is $50m$

Our main interest is in the Z component of the wind. In table 2 some statistical properties of the Z component of wind as function of the flight forward velocity are presented.

It should be noted that in reality, wind conditions do not change by flight conditions, of course, but the results here are sufficiently close for our approximation. Figure 5 shows the spectrum of the wind in direction z. It can be seen that the signal has most of its frequencies lower than 0.3 Hz, indicating that a representing time scale of it is about 3s.

Table 3 shows the same data for wind as in table 2, but for wind velocity in 6 m of 10 m/s. It can be seen that, as expected, the velocities are bigger here.

Velocity (m/s)	W_z mean (m/s)	W_z std (m/s)	max velocity (m/s)
2	-0.0004	0.3412	1.02
4	-0.0012	0.3909	1.17
6	-0.0014	0.4154	1.25
8	-0.0015	0.4313	1.29

Table 2: Wind properties for different flight velocity. Wind velocity in 6 m is 6 m/s. Results for 150 seconds of simulation.

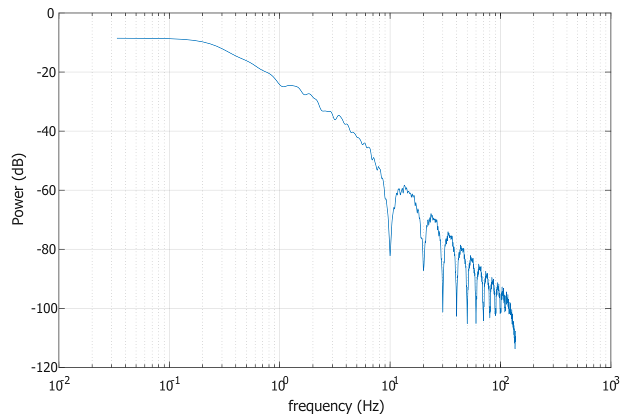

Figure 5: Spectrum of wind in direction z

9 Simulation Results with Wind

After modeling the wind, the effect of it on the controller's performance can be examined. We show here three simulations that were done.

The first simulation is initiated in trim, so without wind, it doesn't change its state. The parameter of wind velocity at 6 m altitude is chosen as 6 m/s, and the quacopter has a velocity of 8 m/s in the x direction (it has an initial pitch angle). The results of the controlled states - z, ψ, θ and ϕ are shown in figure 6.

As can be seen, the wind doesn't affect the errors in euler angles (the errors that are shown in the figure result from numerical errors, and appear also without wind). The error in z is not negligible and oscillates between -1m and 1m. The standard deviation of the error shown in this figure is 0.22m. Figure 7 shows the velocity of the quadcopter in inertial axes. As can be seen, the wind doesn't affect the velocity in the y axes, which is 0, but affects the forward velocity of the quadcopter.

The wind that the rotor experiences is a function not only of the external wind but also the velocity of the quadcopter relative to the air. Hence, it is reasonable to assume that the effect of wind on the velocity in the x direction will be more significant because of the quadcopter forward velocity. This result can also be seen in figure 7.

Velocity (m/s)	W_z mean (m/s)	W_z std (m/s)	max velocity (m/s)
2	-0.0038	0.6821	2.04
4	-0.0069	0.7817	2.33
6	-0.007	0.8315	2.37
8	-0.006	0.8627	2.344

Table 3: Wind properties for different flight velocity. Wind velocity in 6 m is 10 m/s. Results for 150 seconds of simulation.

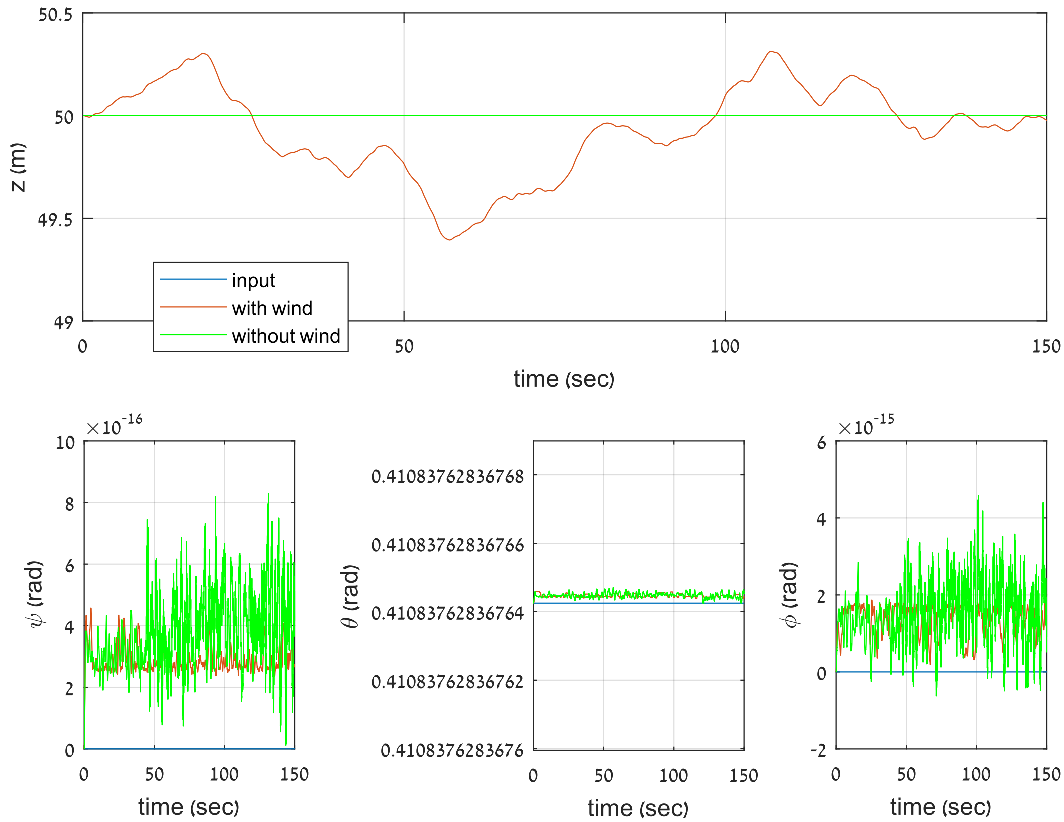

Figure 6: Error of controllers with the presence of wind

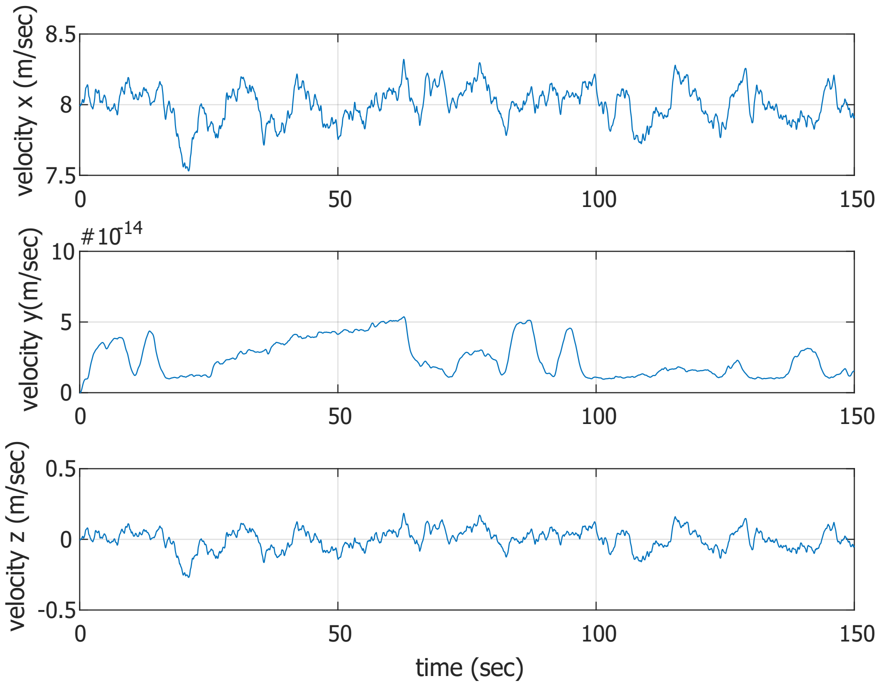

Figure 7: Velocity of the quadcopter with the presence of wind

A comparison of the controller performance in the presence of wind, for different quadcopter velocities is shown in table 4. It can be seen that in fast speed, the error generally decreases. The mean of the error in all velocities is about 0.1 m/s. For change in the parameter of the wind velocity at 6m, the comparison is showed in table 5.

Forward velocity (m/s)	z error std (m)
2	0.2178
4	0.2695
6	0.2861
12	0.2496
20	0.1874

Table 4: Standard deviation of error for different forward velocities. Wind speed at 6m is 6m/s

Wind speed at 6m	z error std (m)
2	0.0822
6	0.2496
10	0.4214
15	0.6425

Table 5: Standard deviation of error for different wind states. Quadcopter forward velocity is 12 m/s

The second and third simulations are of quadcopter that starts in trim with 10 m/s forward velocity, and again, wind speed at 6m of 6m/s. The second simulation has a altitude command after 5 seconds and roll command after 30 seconds. The results are shown in figure 8. As can be seen, the wind has almost no effect on the attitude of the quadcopter. The effect of the wind on the altitude is similar to the one in the first simulation.

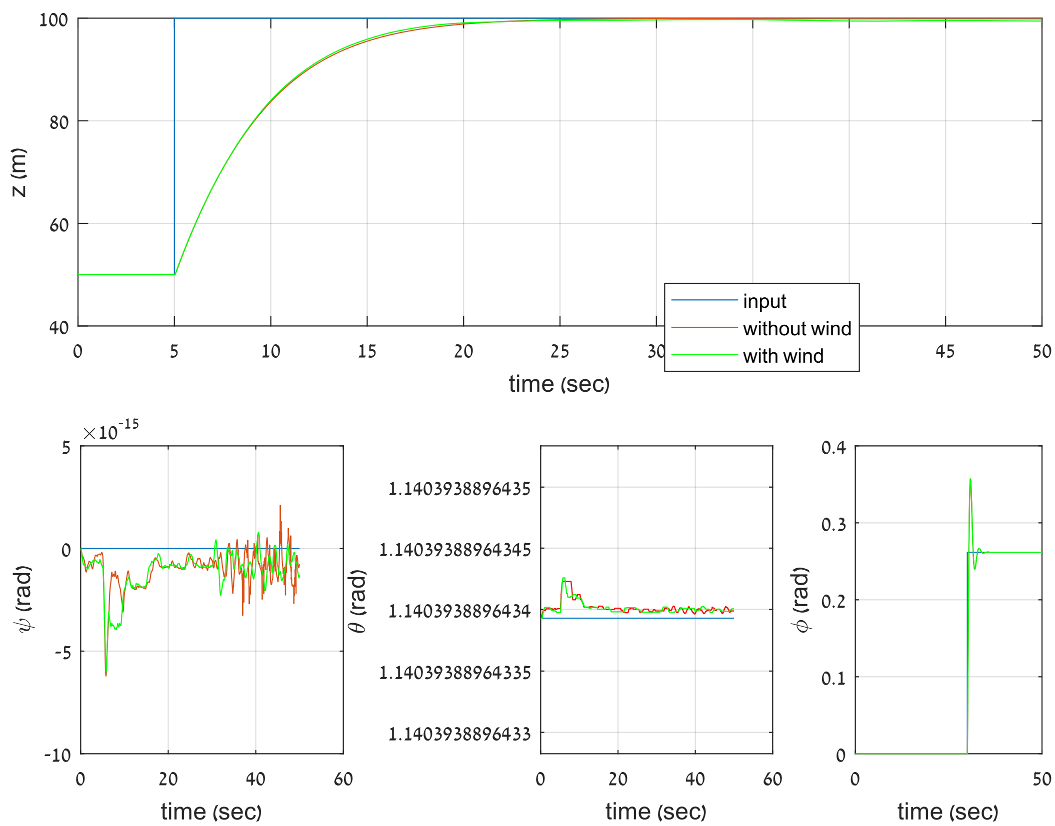

Figure 8: Second simulation results

The third simulation has a sinusoidal command on ψ with 2 degrees amplitude, and a 10m command on z. As can be seen in figure 9, the loop on ψ almost doesn't have gain and phase difference. The value of ϕ becomes sinusoidal although there is no command for it. However, it seems that the wind has a minimum effect on the results, and only the z location of the quadcopter oscillates more than in the quite scenario. Figure 10 shows the velocity of the quadcopter with the presence of wind. It is evident that the effect of wind is negligible.

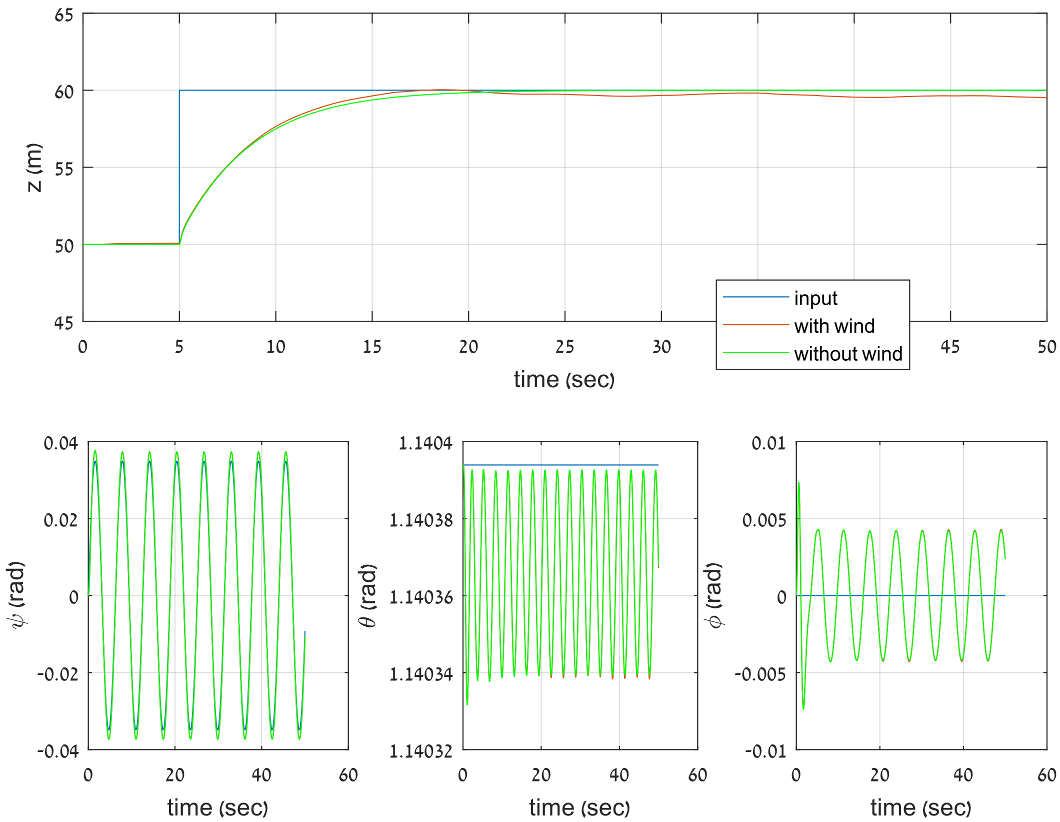

Figure 9: Third simulation results

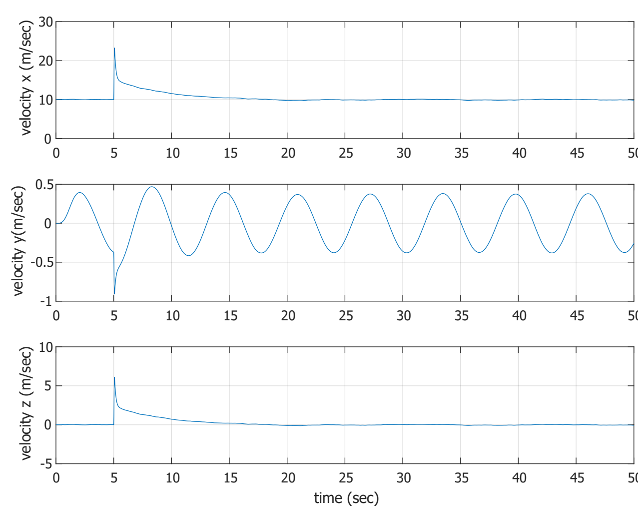

Figure 10: Velocity of quadcopter in the third simulation

9.1 Monte Carlo simulations

In order to characterize the process, a monte carlo simulation with 300 simulations was run. The simulations were of 100 seconds, for a quadcopter in trim with 10 m/s forward velocity at 50 m altitude, and wind that has 6 m/s velocity in 6 m altitude.

The standard deviation of each of the simulations in each time, after a short transient, is almost constant, as can be seen in figure 11.

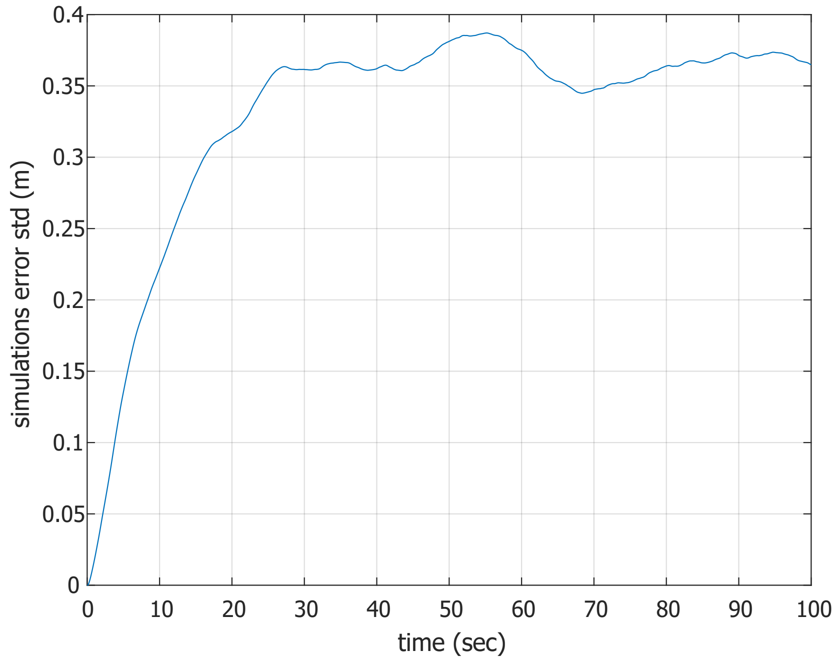

Figure 11: Ensemble standard deviation of the simulation

However, taking the standard deviation of the error in altitude in each run (time-average) starting in second 30 (after the transient), we get 0.247m in average with standard deviation of 0.092m. The error standard deviation for each simulation is shown in figure 12. It can be seen that it is not stable and varies from run to run. In addition, the standard deviation of single run error does not match ensemble standard deviation in time. From these results we conclude that the process is not ergodic. It can be that performing more simulations in the monte carlo simulation, and simulating a longer scenario will change this conclusion. However, it is more reasonable to assume that the strong wind makes the system to behave not linearly so the process is not ergodic.

From the fact that the standard deviation of the error in time reaches steady state after a short time comes to the conclusion that the process is stationary. Although the average in each time is not constant, it varies around 0 with an amplitude that is order of magnitude smaller, so it is probably due to short simulation time and small number of simulations.

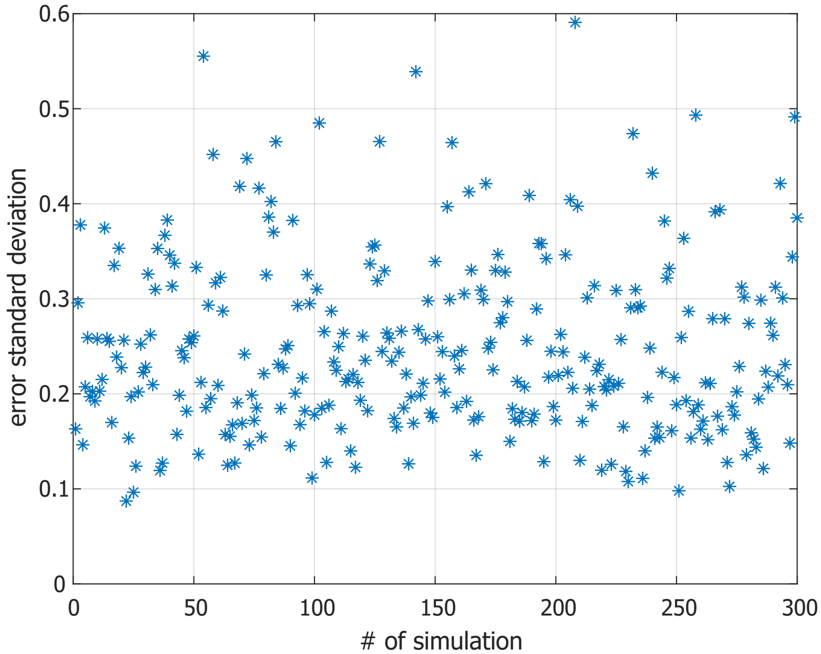

Figure 12: Error standard deviation for each simulation in MC run

10 Conclusions

A quadcopter can be stabilized by a simple PD controller. However, a presence of wind causes the loop on the altitude of the quadcopter to oscillate, and it doesn't achieve steady state. However, the results in this report show that the disturbance is not fatal, and the altitude is close to constant. The tool that was developed in this report can be used in future to check the performance of more complicated controllers, as the ground tracking controller that is based on laser. A reasonable hypothesis is that it will be possible to track the altitude above ground with some tolerance. An interesting question to be studied is what is the relation between the wind parameters and the oscillations of the altitude.

References

[Luukkonen, 2011] T. Luukkonen, Modelling and control of quadcopter, School of Science, Espoo, August 22, 2011

[Hoblit, 1998] F.M. Hoblit, Gust Loads on Aircraft: Concepts and Applications, AIAA Education Series, 1998

[Iosilevskii] G. Iosilevskii, Technical report on rotor torque